GEOPHYSICAL RESEARCH LETTERS, VOL. 26, NO. 24, PAGES 3697-3700, DECEMBER 15, 1999

Spatio-temporal analysis of stress diffusion in a mining-induced seismicity system

David Marsan, Christopher J. Bean

Geology Department, University College Dublin, Ireland

Sandy Steacy, John McCloskey

School of Environmental Studies, University of Ulster, Coleraine, N. Ireland

Abstract. The spatio-temporal correlation of micro-earthquakes occuring in a mining-induced seismic system (Creighton mine, Ontario, Canada) is investigated. It is shown that, when considering only the after-events correlated to a main event, i.e., not accounting for the uncorrelated regime of 'background' activity, the spatial distribution of these after-events occuring at t after the main event change with t. This change takes the form of an expanding pattern, characterized by a typical scale $L_c(t)$ varying as $L_c(t) \sim t^H$, H being estimated to 0.18. This diffusion exponent is found to increase when considering only a subset of the most energetic events as mainshocks. We interpret this result as the indication of a stress (sub-)diffusion mechanism, involving propagation on the heterogeneous fractal fault network.

1. Introduction

It is well known that seismicity patterns vary in both space and time. In space, the clustering of epi/hypocenters for small to large areas has been found to possess a fractal [*Kagan and Knopoff*, 1980; *Okubo and Aki*, 1987] or multifractal [*Geilikman et al.*, 1990; *Hirata and Imoto*, 1991; *Hirabayashi et al.*, 1992; *Lei et al.*, 1993; *Hooge et al.*, 1994; *Wang and Lee*, 1996] nature, therefore no characteristic scale within a scaling range can be singled out. It is often suggested that this is associated with the fractal or multifractal distribution of faults on which the seismic activity occurs.

Regarding the clustering in time, we can go back to Omori's work [*Omori*, 1895] on the decay with time t of the rate of aftershocks $n(t)$, which corresponds (in the modified Omori's law form $n(t) \sim t^{-p}$) to a temporal fractal clustering with dimension $1-p$. This clustering is normally found at relatively small time scales, but characterizes all sizes of seismic systems, from acoustic emissions (AE) in rock samples [*Hirata*, 1987] to earthquakes of large magnitudes. It is seen as a local readjustement of the system following a perturbation of its stress field.

Despite the clear evidence that clustering in both space and time characterize seismicity, these two types of clustering are usually investigated separately. However, it can be expected that the study of space-time correlations in seismicity systems will help to link these two phenomena, and will therefore help to study the underlying dynamics of earthquake populations. Two types of processes with space-time scaling can be distinguished: one where there are no interactions between the spatial and temporal domains, leading to trivial dynamics [*Shaw*, 1993], and another with space-time interactions, therefore introducing non-trivial dynamics. The latter case is ubiquitous in physics and geophysics. For example, growth processes verifying the Family-Vicsek scaling [*Family and Vicsek*, 1985] are scaling in both space and time, associating to all spatial scales ℓ a characteristic time scale $t \sim \ell^Z$. This is also relevant to turbulence, and goes back to the idea of *Richardson* [1922] of a cascade of structures or 'turbulent eddies' at all scales, possessing typical life-times. Exploiting the work of *Kolmogorov*, [1941], one gets that, for turbulence, $t \sim \ell^{2/3}$.

For seismicity systems, the very fact that clustering is observed both in space and time should make us aware of the possible existence of a stress diffusion phenomenon, corresponding to a propagation of the stress away from the initial earthquake, at time scales much larger than those involved in seismic wave propagation. Such a diffusion phenomenon has been reported or predicted in many papers. Expansion patterns of aftershock areas following large earthquakes, mostly in subduction zones, have for example been described [e.g., *Mogi* 1968]. *Tajima and Kanamori* [1985] quantified these expansions by defining an expansion ratio, indicating rather slow propagation processes. Mechanical models of subduction zones have been proposed, ellaborating on the model of *Elsasser* [1969] who predicted a stress diffusion similar to the classical heat diffusion, due to the coupling between an elastic lithosphere lying on top of a fluid asthenosphere. Such a stress diffusion would characterize large faults or subduction arcs, for which a clear migration of earthquakes along such structures is observable. Propagation of individual strain/stress perturbations have been recently reported by *Malin and Alvarez* [1992] along the San Andreas fault, by *Grasso et al.* [1992] in the Pyrenean fault zone, by *Sanders* [1993] along the San Jacinto fault zone, and by *Mantovani and Albarello* [1997] through the Adriatic plate. Other studies have also documented general statistical trends in space-time clustering of earthquakes, which could indicate the existence of local diffusion mechanisms [*Ouchi and Uekawa*, 1986; *Eneva and Pavlis*, 1991].

In this paper, we analyze the spatio-temporal distribution of micro-earthquakes occuring in an underground mine (Creighton mine, Ontario, Canada), in order to determine whether a stress diffusion is active for this system or not. The methodology we follow corresponds to analyzing how the occurence of an earthquake perturbs the stress field.

Paper number 1999GL010829.
0094-8276/99/1999GL010829$05.00

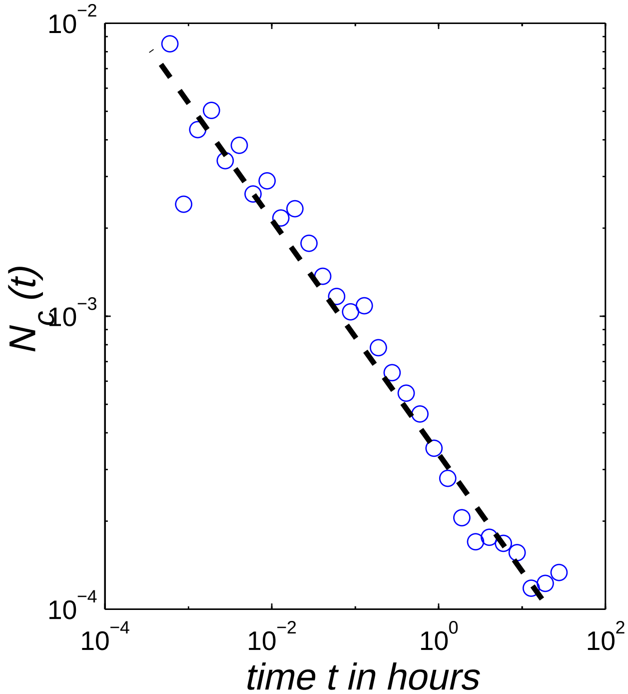

Figure 1. Number of correlated events $N_c(t)$ occuring at t after the main event. The dashed line indicates a power law with an algebraic exponent of -0.4.

The temporal evolution of this perturbation is then taken as corresponding to the changes with time of the spatial distribution of the afterevents 'triggered' by the initial perturbation. A diffusion process would manifest itself by an average migration of these afterevents away from the initial earthquake, therefore changing the spatial structure of the perturbation by enhancing the larger spatial scales.

2. Analysis of the spatio-temporal patterns in the microseismicity of Creighton Mine

2.1. Data

We analyze the space-time correlation of the microseismicity recorded in Creighton Mine, Ontario, Canada, between the 1st of October 1997 and the 31st of March 1998. We use the dataset consisting of $\mathcal{N}$ =10733 events provided by the Queen's Microseismic System (QMS) full waveform data network located in the deeper levels of the mine (at about 2000 m depth), a micro-earthquake triggering between 0 and 5 triaxial and between 5 and 29 uniaxial sensors. The network underwent a 43-hour shutdown between the 29th and the 31st of December 1997, but otherwise was permanently recording the seismic activity. This seismicity is induced by the mining activity, the region being otherwise seismically quiescent. The seismically active volume of the mine, as recorded by the network, has a size of the order of 500^3 m^3, and the error on the location of the micro-earthquakes is typically around 17 m, as given by averaging over the estimates of the location errors computed during the processing of the seismic signals. The temporal resolution is 1 s. These data are provided along with a measure of the magnitude. However, cut-offs at small magnitude (resolution of the network) and, more importantly, at large magnitude (saturation of the seismograms) limit the properly resolved range to about 1.5 orders of magnitude.

2.2. Time clustering

We first define as the 'main event' the earthquake for which the clustering, either in space, time, or both, is determined, regardless of its magnitude. Also, we define the 'after events' as all the earthquakes following the main event, in time. Denoting by t_i the time of occurence of the i^{th} earthquake, we compute the average number $N(t)$ of afterevents occuring at a delay t after the main event as $N(t) = \frac{1}{\mathcal{N}} \sum_{i=1}^{\mathcal{N}} \sum_{j/t_j>t_i} \Theta(t_j - t_i \in [t; t+\tau])$ where $\Theta(t \in I)$ is 1 if $t \in I$, 0 otherwise, $\mathcal{N}$=10733 is the total number of events, and τ =1 s is the resolution scale. The number $N_c(t)$ of correlated afterevents at delay t is obtained by substracting the average number of events $\bar{n}_\tau$ occuring in an interval of duration τ from $N(t)$: $N_c(t) = N(t) - \bar{n}_\tau$. Here $\bar{n}_\tau = 6.9\ 10^{-4}$ events/second. A temporally uncorrelated population of micro-earthquakes would be such that $N(t) = \bar{n}_\tau$, at all t. Figure 1 shows $N_c(t)$, averaged on an algebraic set of times t varying from 1 s to 1 week. It scales as $N_c(t) \sim t^{-p}$ with $p = 0.4$ over more than 4 decades. The relatively low value of p reflects a weak clustering on average, compared to what is traditionally observed for larger tectonics systems with p generally close to 1, a difference probably due to the different type of correlation examined (only large earthquakes are typically considered as main shocks when classically determining a p-value). For $N(t)$, two dynamical regimes can be distinguished: (i) a correlated regime at

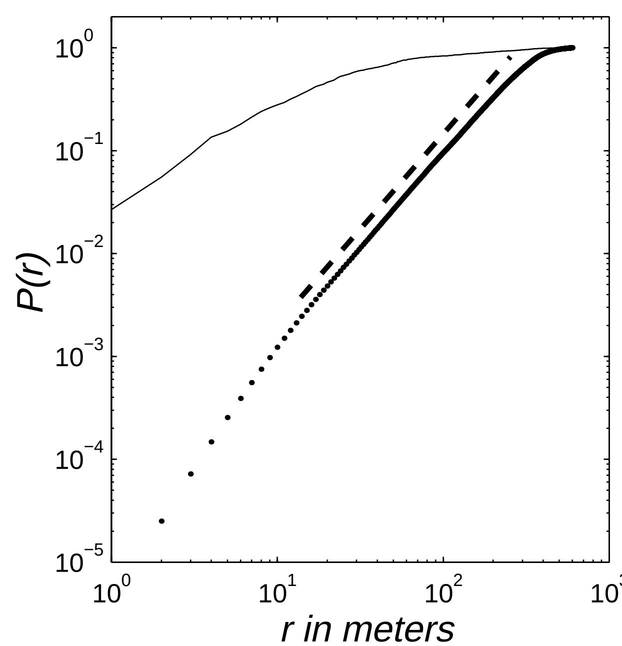

Figure 2. Probability $P(r)$ of an event occuring within a distance r away from the main event. Continuous line: pairs of events occuring within 10 s of each other. Dots: all pairs of events. Dashed line: power law with algebraic exponent 1.85. Note for the dotted curve a change of slope at scales smaller than the error scale at 17 m, indicative of a near-to-random distribution at such scales.

short time scales (up to about 1 hour), for which $N_c(t)$ is larger or comparable to $\bar{n}_\tau$, and (ii) an uncorrelated regime at time scales longer than one hour, for which $N_c(t)$ becomes negligible compared to $\bar{n}_\tau$, i.e., $N(t) \simeq \bar{n}_\tau$.

2.3. Spatial clustering

We compute the correlation integral [*Grassberger and Procaccia*, 1983] of the micro-earthquakes, assuming an isotropic scaling in the three spatial directions (Figure 2). Both the small size of the active part of the mine and the spatial resolution of the network at 17 m limit the scaling range to little more than one decade, from 17 m to about 250 m, yielding the fractal dimension $D = 1.85$. For any earthquake, taken as a main event, the spatial structure revealed by the correlation integral corresponds to the structure of the temporally uncorrelated regime (cf. section 2.2), since it is computed at the maximum scale available (6 months), much larger than the transition scale at 1 hour.

The spatial clustering of the afterevents following a main event at very short time scales (less than 10 s) differs greatly from the one at large time scales. In figure 2 we compare the two: at short time scales, the spatial distribution is dominated by the temporally correlated regime, and is significantly more clustered around the main event. No obvious scaling is observed for this regime.

2.4. Temporal evolution of the mean distance between pairs of correlated events

In order to test the existence of a diffusion process characterizing the temporally correlated regime, we determine the mean distance $L_c(t)$ between pairs of temporally correlated events (section 2.2) separated by a delay t. This can be done by first computing the mean distance $L(t)$ between any pairs of events separated by t, which is the sum of the two contributions: (i) from the temporally correlated events, $\frac{N_c(t)}{N(t)}L_c(t)$, and (ii) from the temporally uncorrelated events, $\frac{\bar{n}_\tau}{N(t)}\bar{L}$, where $\bar{L} = 273$ m is the mean distance between any pair of events. Figure 3 shows that $L_c(t)$ follows a power law $L_c(t) \sim t^H$ from about 1 s to the transition scale at 1 hour, H being estimated to 0.18. For time scales larger than 1 hour, $L_c(t)$ grows significantly more slowly.

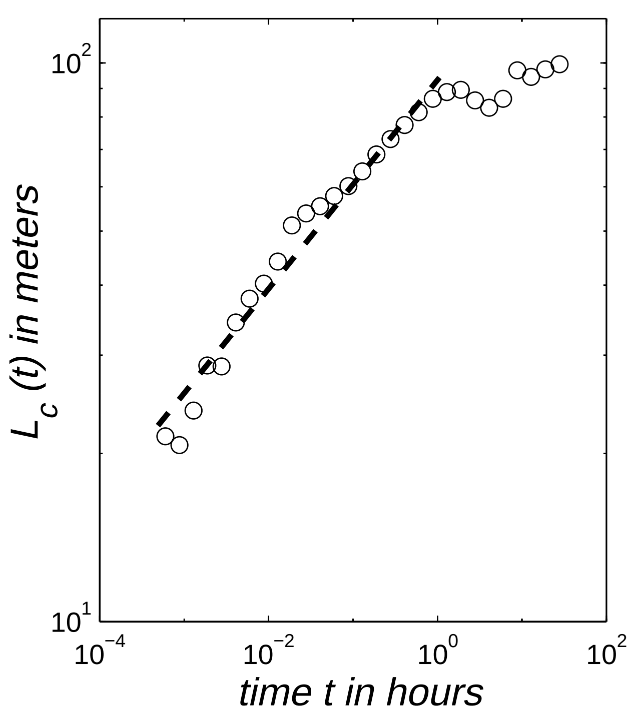

Figure 3. Mean distance $L_c(t)$ between temporally correlated events separated by a delay t. The dashed line gives an algebraic exponent equals to 0.18.

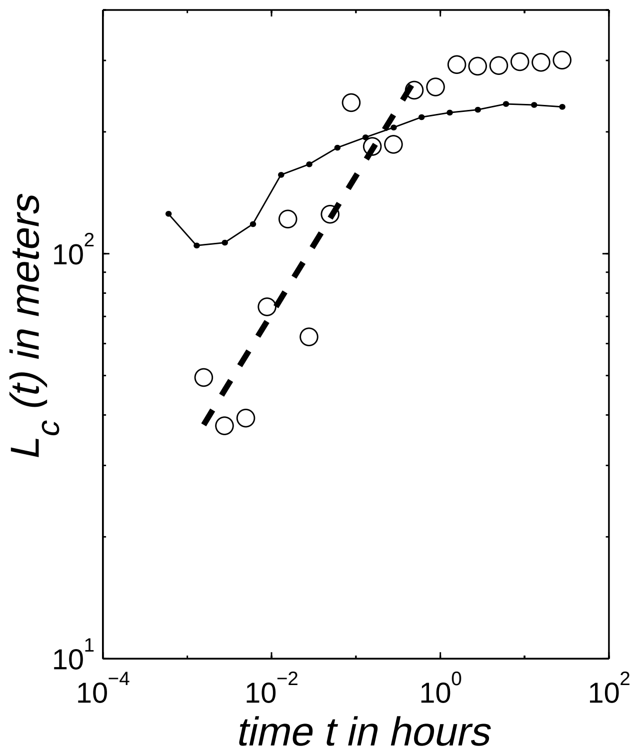

Figure 4. Mean distance $L_c(t)$ between temporally correlated events separated by a delay t, for the two subsets of main events: (1) continuous line: small events, and (2) dashed line: large events. The dashed line gives an algebraic exponent equals to 0.34. See text for a definition of the 'small' and 'large' events.

We reproduced (figure 4) this analysis but now selecting as main events (1) the 146 large events that saturated the measuring network, and (2) the 2909 small events for which the network could not determine a magnitude. For the large events, the diffusion is found to be faster ($H = 0.34$) than the one characterising all events (figure 3), while the spatial expansion of afterevents following the small events is very slow, with no obvious scaling behavior.

3. Discussion and conclusion

We have identified and quantified a stress diffusion mechanism in a seismically active mine. The spatial structure of the temporally correlated regime tends to enhance the larger scales with time, resulting in a growth of the mean distance $L_c(t)$. Also, such a growth is faster when considering the most energetic earthquakes. These observations could be explained by modeling this seismicity system as a scale-invariant ensemble of connected faults on which individual stress concentrations undergo spatial relaxations (through propagation) similar to random walks. The increase of H with the increase in energy release of the main event might be due to the fractal dimension of the fault network being locally smaller in zones that can support larger strain accumulations; this multifractality of the fault network would then correspond to a more efficient propagation, and therefore spatial relaxation, of large stress concentrations/singularities.

An interesting question would be whether this mechanism can be found for 'natural' seismicity systems, and also whether the value of H depends on the regional/local crustal properties. For example, as is proposed above, H might be strongly dependent on the geometry of the local fault network.

Acknowledgments. The authors thank an anonymous referee and J. R. Grasso for helping in improving and clarifying the manuscript. DM and SS were funded by the International Nickel Company, owner of Creighton Mine, which also provided the data.

References

Elsasser W. M., Convection and stress propagation in the upper mantle, in *The application of modern physics to the Earth and planetary interiors*, ed. S. K. Runcorn, Wiley-Interscience, 1969.

Eneva M., and G. L. Pavlis, Spatial distribution of aftershocks and background seismicity in central California, *PAGEOPH*, **137**, 35, 1991.

Family F., and T. Vicsek, Scaling of the active zone in the Eden process on percolation networks and the ballistic deposition model, *J. Phys. A*, **18**, L75, 1985.

Geilikman M. B., T. V. Golubeva, and V. F. Pisarenko, Multifractal patterns of seismicity, *Earth Plan. Sci. Lett.*, **99**, 127, 1990.

Grassberger P., and I. Procaccia, Characterization of strange attractors, *Phys. Rev. Lett.*, **50**, 346, 1983.

Grasso J. R., J. P. Gratier, J. F. Gamond, and J. C. Paumier, Stress transfer and seismic instabilities in the upper crust - Example of the western Pyrenees, *J. Struct. Geol.*, **14**, 915, 1992.

Hirabayashi T., K. Ito, and T. Yoshii, Multifractal analysis of earthquakes, *PAGEOPH*, **138**, 591, 1992.

Hirata T., Omori's power law aftershock sequences of microfracturing in rock fracture experiment, *J. Geophys. Res.*, **92**, 6215, 1987.

Hirata T., and M. Imoto, Multifractal analysis of spatial distribution of microearthquakes in the Kanto region, *Geophys. J. Int.*, **107**, 155, 1991.

Hooge C., S. Lovejoy, D. Schertzer, S. Pecknold, J.-F. Malouin, and F. Schmitt, Multifractal phase transitions: The origin of self-organized criticality in earthquakes, *Nonl. Proc. Geophys.*, **1**, 191, 1994.

Kagan Y., and L. Knopoff, Long-term earthquake clustering, *Geophys. J. R. Astr. Soc.*, **62**, 303, 1980.

Kolmogorov A. N., Local structure of turbulence in an incompressible liquid for very large Reynolds numbers, *C. R. Aca. Sci. USSR*, **30**, 299, 1941.

Lei X., O. Nishizawa, and K. Kusunose, Band-limited heterogeneous fractal structure of earthquakes and acoustic-emission events, *Geophys. J. Int.*, **115**, 79, 1993.

Malin P. E., and M. G. Alvarez, Stress diffusion along the San-Andreas fault at Parkfield, California, *Science*, **256**, 1005, 1992.

Mantovani E., and D. Albarello, Medium-term precursors of strong earthquakes in southern Italy, *Phys. Earth Planet. Int.*, **101**, 49, 1997.

Mogi K., Sequential occurences of recent great earthquakes, *J. Phys. Earth*, **16**, 30, 1968.

Okubo P. G., and K. Aki, Fractal geometry in the San Andreas fault system, *J. Geophys. Res.*, **92**, 345, 1987.

Omori F., On the aftershocks of earthquakes, *J. Coll. Sci.*, **7**, 111, 1895.

Ouchi T., and T. Uekawa, Statistical analysis of the spatial distribution of earthquakes - Variation of the spatial distribution of earthquakes before and after large earthquakes, *Phys. Earth Planet. Int.*, **44**, 211, 1986.

Richardson L. F., *Weather prediction by numerical processes*, republished by Dover (1965), 1922.

Sanders C. O., Interaction of the San-Jacinto and San-Andreas fault zones, southern California - Triggered earthquake migration and coupled recurrence intervals, *Science*, **260**, 973, 1993.

Shaw B. E., Generalized Omori law for aftershocks and foreshocks from a simple dynamics, *Geophys. Res. Lett.*, **20**, 907, 1993.

Tajima F., and H. Kanamori, Global survey of aftershock area expansion patterns, *Phys. Earth Plan. Int.*, **40**, 77, 1985.

Wang J.-H., and C.-W. Lee, Multifractal measures of earthquakes in west Taiwan, *PAGEOPH*, **146**, 131, 1996.

D. Marsan and C. J. Bean, Department of Geology, University College Dublin, Belfield, Dublin 4, Ireland. (e-mail: david.marsan@ucd.ie, chris.bean@ucd.ie)

S. Steacy and J. McCloskey, School of Environmental Studies, University of Ultser, Coleraine, Co. Derry, N. Ireland, BT52 1SA (e-mail: s.steacy@ulst.ac.uk, j.mccloskey@ulst.ac.uk)

(Received May 11, 1999; revised August 26, 1999; accepted August 31, 1999.)